Proc. Natl. Acad. Sci. USA
Vol. 92, pp. 8574–8578, September 1995
Genetics

Subunit-destabilizing mutations in *Drosophila* copper/zinc superoxide dismutase: Neuropathology and a model of dimer dysequilibrium

JOHN P. PHILLIPS*†, JOHN A. TAINER‡, ELIZABETH D. GETZOFF‡, GABRIELLE L. BOULIANNE§, KIM KIRBY*, AND ARTHUR J. HILLIKER*

*Department of Molecular Biology and Genetics, University of Guelph, Guelph, ON Canada N1G 2W1; ‡Department of Molecular Biology, The Scripps Research Institute, La Jolla, CA 92037; and §Department of Physiology and Centre for Research in Neurodegenerative Diseases, University of Toronto, Toronto, ON Canada M5S 1A8

Communicated by Irwin Fridovich, Duke University Medical Center, Durham, NC, May 18, 1995 (received for review March 1, 1995)

ABSTRACT **Mutations in Cu/Zn superoxide dismutase (SOD), a hallmark of familial amyotrophic lateral sclerosis (FALS) in humans, are shown here to confer striking neuropathology in *Drosophila*. Heterozygotes with one wild-type and one deleted SOD allele retain the expected 50% of normal activity for this dimeric enzyme. However, heterozygotes with one wild-type and one missense SOD allele show lesser SOD activities, ranging from 37% for a heterozygote carrying a missense mutation predicted from structural models to destabilize the dimer interface, to an average of 13% for several heterozygotes carrying missense mutations predicted to destabilize the subunit fold. Genetic and biochemical evidence suggests a model of dimer dysequilibrium whereby SOD activity in missense heterozygotes is reduced through entrapment of wild-type subunits into unstable or enzymatically inactive heterodimers. This dramatic impairment of the activity of wild-type subunits *in vivo* has implications for our understanding of FALS and for possible therapeutic strategies.**

Mutations in Cu/Zn superoxide dismutase (SOD, EC 1.15.1.1) have been identified in the etiology of familial amyotrophic lateral sclerosis (FALS), a syndrome commonly known as Lou Gehrig's disease (1, 2). Some FALS-affected individuals are carriers of missense mutations that appear to alter the stability (3) and/or the function of this critical oxygen radical-metabolizing enzyme (2). The dominant phenotype associated with FALS mutations in SOD could result from loss of enzyme function, consistent with the reduced SOD activity in FALS patients (2, 4–7), or from the gain of a deleterious function, such as enhanced reactivity with peroxynitrite leading to elevated protein-tyrosine nitration (8, 9), consistent with the motor neuron damage found in transgenic mice overexpressing FALS-type mutant SOD (10, 11).

A direct test of the relationship between SOD subunit function and neurodegenerative disease would be to induce and select mutations in SOD in an organism amenable to genetic analysis and then characterize the biochemical and neurological consequences conferred by these mutations. We have previously shown that null mutation for SOD in *Drosophila melanogaster* confers a syndrome including reduced adult lifespan, infertility, toxic hypersensitivity to a variety of oxygen stress conditions, and lethality in combination with mutations conferring defects in other oxygen radical scavengers (12–16). Overt symptoms of the SOD-null syndrome have been described only in homozygotes and are ameliorated by *P* element-vectored SOD transgenes (ref. 17; T. Parkes, A.J.H., and J.P.P., unpublished data).

Here we show that mutations in SOD in *Drosophila*, as in humans, cause neuropathology. We also show that missense mutations expected to destabilize SOD subunits and dimer assembly significantly impair the activity of normal subunits in heterozygotes for a wild-type allele, resulting in significantly lower enzyme activity than expected in heterozygotes. These findings are important to our understanding of the causative relationship between mutation in SOD and FALS-type neuropathology.

MATERIALS AND METHODS

***Drosophila* Mutants.** Mutations were generated by mutagenizing genetically marked chromosomes bearing SOD^F or SOD^S alleles with ethyl methanesulfonate (EMS), γ irradiation, or hybrid dysgenesis. SOD^F and SOD^S are naturally occurring alleles which specify electrophoretically fast and slow migrating forms of SOD, respectively (18, 19). The SOD^S allozyme differs from the more common SOD^F allozyme by a single amino acid change ($Asn^{96} \rightarrow Lys$). Mutant alleles *n108, x16,* and *x39* were generated in our laboratory (Guelph); alleles *n58, n64, n83,* and *n145* were generated in the laboratory of the late Glen Bewley. Previous work on *n108* and *Df(3L)h76* is described elsewhere (12–16). Mutants were initially identified as recessive adult lethals or semilethals in selectable genetic backgrounds and screened for activity as heterozygotes with the appropriate SOD^F or SOD^S "counterallele." Other genetic markers and chromosomes are described in ref. 20.

Histology. For horizontal sections, fly heads were dissected and probosci were removed. Heads were fixed in 2% formaldehyde/2% glutaraldehyde/0.01 M phosphate at pH 7.2, prepared for paraffin histology, serially sectioned at 6 μm, and stained as described (21). Tangential sections were processed as above with the exception that the heads were bisected prior to fixation to allow better infiltration of fixative.

SOD Activity Assay. Extracts were prepared and assayed for SOD activity either directly (13) or following nondenaturing polyacrylamide gel electrophoresis (22).

DNA Sequencing. *SOD* alleles were analyzed by dideoxy sequencing of at least two independent PCR amplifications of the two constituent exons of the *Drosophila SOD* gene (23). Total PCR errors detected by sequencing were <0.1%. PCR primers used in sequencing were as follows: for exon 1, 5′-TAA-ATT-GAT-TAA-TTC-ATT-CG-3′ and 5′-CAA-ATG-ATT-TTG-GAT-TCT-CAC-3′, and for exon 2, 5′-TCC-CCT-CAT-CCC-GTC-CAC-AG-3′ and 5′-ACA-TCG-GAA-TAG-ATT-ATC-GC-3′. PCR-amplified genomic DNA was subcloned into pBluescript KS (Stratagene) and sequenced with the T7 sequencing kit (Pharmacia).

The publication costs of this article were defrayed in part by page charge payment. This article must therefore be hereby marked "*advertisement*" in accordance with 18 U.S.C. §1734 solely to indicate this fact.

Abbreviations: SOD, superoxide dismutase; FALS, familial amyotrophic lateral sclerosis; EMS, ethyl methanesulfonate.

†To whom reprint requests should be addressed.

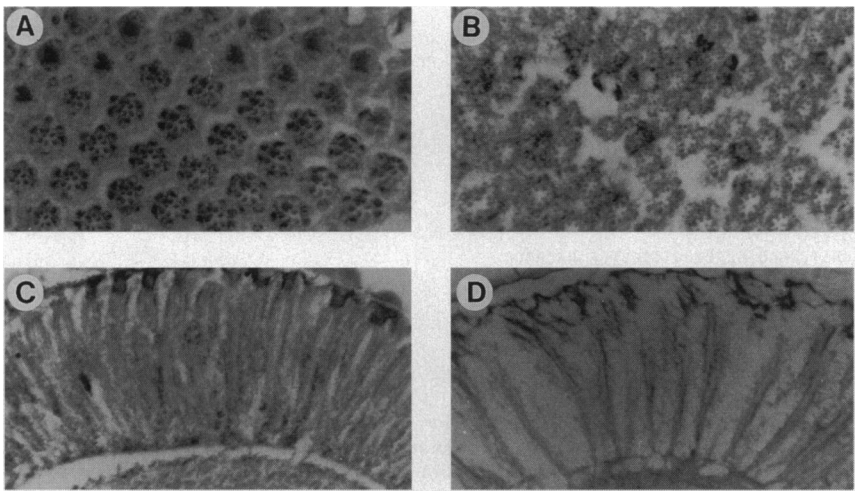

FIG. 1. Histopathology in *SOD*-null mutant adults. Shown are 6-μm paraffin sections of compound eyes of 7-day-old adults stained with toluidine blue. (*A*) Tangential section through an eye of a SOD^{+} homozygote showing the regular array of ommatidia. (*B*) Tangential section through an eye of a SOD^{n108} homozygote illustrating general internal disorganization of the ommatidial array. Lesions between ommatidia, indicative of cell atrophy, are apparent. In the ommatidia which remain, the complement of photoreceptor neurons and pigment cells is varied and often disorganized; the rhabdomeres appear smaller and shrunken than in the wild-type homozygote. (*C*) Horizontal section through an eye of a SOD^{+} homozygote at the level of the retina. As in *A*, the axonal projections from the photoreceptor cells are complete and arranged in a regular array with no apparent gaps. (*D*) Horizontal section through an eye of a SOD^{n108} homozygote at the level of the retina. As in *B*, large lesions can be seen throughout the retina, indicative of necrosis and cell loss.

RESULTS AND DISCUSSION

Neuropathology. Histological examination of the visual system of homozygous SOD^{n108} adults reveals extensive necrotic lesions throughout the retina (Fig. 1). Atrophy and necrosis affect several ommatidial cell types, principally photoreceptor neurons; primary and secondary pigment cells are also missing or necrotic. The normal crystalline array of corneal facets exhibited by the mutant eye suggests that the histopathology arises after the major cell types of the eye are formed during metamorphosis. Histological defects in the photoreceptor neurons of the mutant retina also extend into the adjacent lamina of the brain (G.L.B., A.J.H. and J.P.P., unpublished data). Such neuropathology is consistent with behavioral defects—including reduced motor activity, recently observed for this mutant (D. Dickinson, A.J.H., and J.P.P., unpublished data)—and demonstrates the important role of SOD in the nervous system of *Drosophila*.

Molecular Analysis of *SOD* Null Mutations. *Drosophila* provides a useful genetic system to analyze the *in vivo* relationship among *SOD* mutations, subunit function, and neuropathology. To this end, we determined the molecular lesions in a set of induced mutant alleles of *Drosophila SOD* (Table 1). These alleles, in contrast to human FALS alleles, were generated experimentally by ionizing radiation or EMS and selected on the basis of enzymatic defects in SOD. Two deletion alleles and five missense alleles were analyzed. Both deletion alleles were generated by ionizing radiation and are unable to encode SOD subunits: *x16* has an 11-bp out-of-frame deletion in the first exon, whereas *x39* has a 395-bp deletion encompassing the transcription start site, all of the first exon, and part of the single intron.

Mutation sites on *Drosophila* SOD were mapped onto a homology model of the *Drosophila* enzyme generated from published crystallographic structures of bovine (24) and human (25, 26) SOD as well as from structures of bovine and yeast SOD now refined at 1.8-Å and 1.7-Å resolution, respectively (H. Parge, M. Hariharan, S. Redford, D. McRee, and J.A.T., unpublished data). The EMS-generated missense mutations map to two distinctly different structural/functional regions of the protein (Fig. 2). The $Gly^{49} \rightarrow Ser$ mutation of allele *n108* disrupts one of two pairs of symmetric main-chain hydrogen bonds formed across the dimer interface through steric collisions with the newly introduced side-chain atoms. The $Gly^{42} \rightarrow Glu$ (*n64*), $His^{69} \rightarrow Tyr$ (*n83*), and $Gly^{83} \rightarrow Asp$ (*n58*) mutations all disrupt interactions stabilizing the binding of the active-site Cu and Zn ions (see legend to Fig. 2). Besides reducing activity at neutral pH, loss of Zn is expected to destabilize the subunit structure (28). Like the known human FALS mutations, these mutation sites all involve changes to structurally conserved interactions identified in the human, bovine, and yeast SOD crystallographic structures that are expected to destabilize the subunit fold or dimer assembly (Fig. 2). In fact, mutation *n58* alters precisely the same residue ($Gly^{83} \rightarrow Asp$) as does a known human FALS allele ($Gly^{85} \rightarrow Arg$; ref. 1).

SOD Activity in Mutant Heterozygotes. To determine the effects of these mutations on enzymatic activity and subunit interaction, we assayed SOD activity in whole body extracts of heterozygous mutant adults. SOD activity in heterozygotes for

Table 1. Wild-type and mutant alleles of *Drosophila SOD*

Allele	Parent chromosome	Mutagen	Lesion	Cu/Zn SOD activity
SOD^{F}	Oregon R		*	
SOD^{S}	Natural allele		†	
Df(3L)h76	$sr\ e^{s}\ ca\ SOD^{F}$	HD	Multigene deletion	Null
x16	$sr\ e^{s}\ ca\ SOD^{F}$	γ-rays	11-bp deletion	Null
x39	$sr\ e^{s}\ ca\ SOD^{F}$	γ-rays	395-bp deletion	Null
n64	$r^{2}\ SOD^{S}\ p^{p}$	EMS	$Gly^{42} \rightarrow Glu$	Null
n108	$sr\ e^{s}\ ca\ SOD^{F}$	EMS	$Gly^{49} \rightarrow Ser$	Null
n83	$r^{2}\ SOD^{S}\ p^{p}$	EMS	$His^{69} \rightarrow Tyr$	Null
n58	$r^{2}\ SOD^{S}\ p^{p}$	EMS	$Gly^{83} \rightarrow Asp$	Null
n145	$r^{2}\ SOD^{S}\ p^{p}$	EMS	(not determined)	Null

Mutations were generated by mutagenizing genetically marked chromosomes bearing either SOD^{F} or SOD^{S} alleles. Genetic markers and chromosomes are described in ref. 20. HD, hybrid dysgenesis.
*Natural wild-type allele (fast electromorph).
†Natural allele $Asn^{96} \rightarrow Lys$ (slow electromorph).

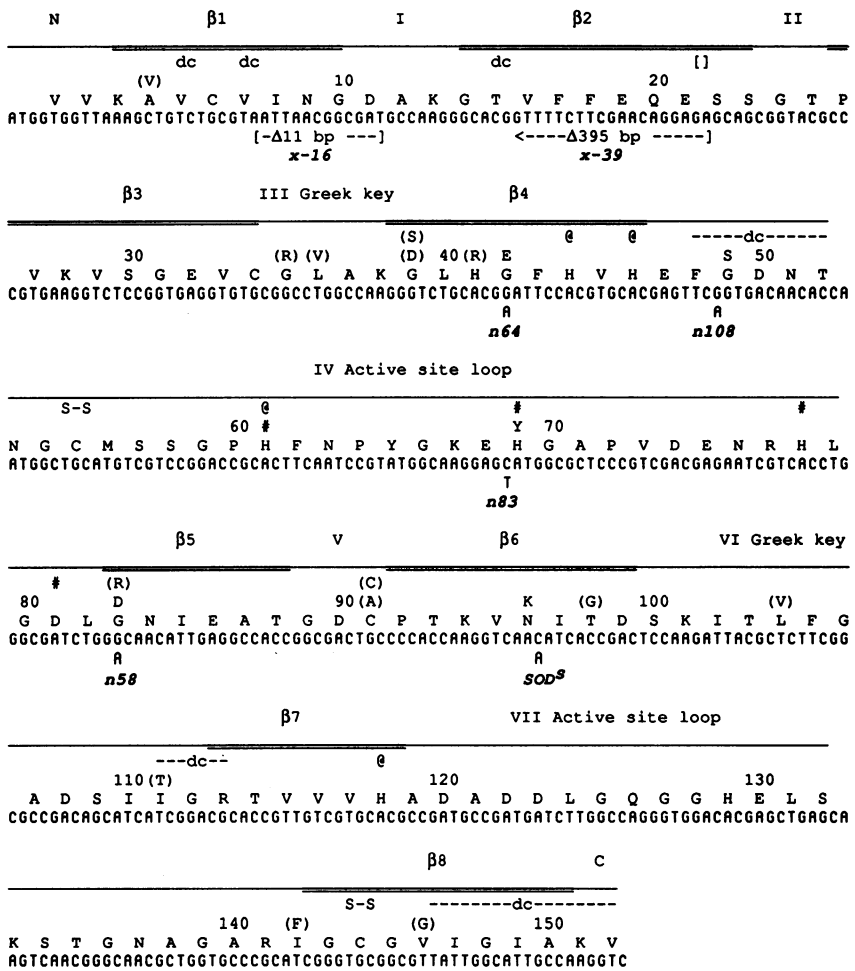

FIG. 2. Mutant lesions mapped to the amino acid and nucleotide sequences of *Drosophila* SOD shown in single-letter codes. Every 10th amino acid residue is numbered. Structural features of SOD, shown above the amino acid sequence, are the eight β-strands of the Greek-key β-barrel (β1–β8), the seven connecting loops (Roman numerals) and N-terminal (N) and C-terminal (C) tails. Sequence alignment and identification of structural features in homologous proteins are from ref. 27. The location of the single intron ([ ]) is also shown. Nucleotide changes in *Drosophila* deletion and missense mutations are indicated below the wild-type nucleotide sequence, and the corresponding amino acid changes are shown above the wild-type amino acid sequence; locations of several human FALS mutations (1, 2) are shown in parentheses. Residues that form disulfide bridges (S-S), ligate Cu (@) or Zn (#), or are predicted to be involved in dimer contact (-dc-) are also shown above the sequence. The *Drosophila SOD* sequence is from ref. 23.

a wild-type allele and one of three deletion alleles, *x16*, *x39*, and *h76*, averages 50% of normal controls (Table 2). This value establishes the base level of SOD activity arising from wild-type homodimers specified by a single-copy wild-type *SOD* gene in a cellular environment with no competing mutant subunits. The 50% value for mutant heterozygotes with one deletion allele also demonstrates the absence of compensating upregulation.

In contrast, heterozygotes for the four missense alleles *n58*, *n64*, *n83*, and *n145* exhibit on average only 13% of normal activity (range, 10.1–14.4%). Theoretically, completely unstable mutant subunits should generate 50% of normal activity in heterozygotes with a wild-type allele (Table 2), while mutant subunits that form stable but enzymatically inactive homodimers and heterodimers should generate 25% of normal activity in heterozygotes with a wild-type allele. The unexpectedly low levels of SOD activity in these missense heterozygotes are consistent with our newly proposed dimer dysequilibrium model (see below), whereby the level of enzymatically active wild-type dimers is reduced through the entrapment of wild-type subunits into very unstable or enzymatically inactive heterodimers. According to this model, activity levels below 25% of normal could arise either by the inability of mutant subunits to form stable homodimers, leading thereby to greater entrapment of wild-type subunits into inactive heterodimers, or by the susceptibility of unstable heterodimers to rapid subunit degradation, reducing thereby the steady-state level of both mutant and wild-type subunits.

Finally, heterozygotes carrying the missense allele *n108* exhibit a distinctly higher level of SOD activity than heterozygotes for the other missense alleles (36.7% versus 13%, respectively, of normal). The location of the *n108* mutation at the dimer interface predicts that it would interfere with dimer stability (see Fig. 3). If this mutation precluded assembly of mutant homo- and heterodimers, *n108* heterozygotes would exhibit 50% of normal activity. Instead, *n108* heterozygotes exhibit somewhat less than 50% activity, suggesting that *n108* subunits can weakly engage wild-type subunits into very unstable or inactive heterodimers.

Interpretation of the above results by the dimer dysequilibrium model predicts that stable, enzymatically active heterodimers will not be found in heterozygotes carrying any of the missense mutations described here. To test this prediction, we generated and analyzed heterozygotes for the presence of enzymatically active homodimers and heterodimers through the use of fast (SOD^F) and slow (SOD^S) electrophoretic alleles of SOD. Heterozygotes carrying a mutant *SOD* allele and a SOD^F or SOD^S counterallele (Table 1) were generated, and the constituent homo- and heterodimeric SOD proteins were separated by nondenaturing polyacrylamide gel electrophoresis and stained for activity (Fig. 4). Active homodimers and SOD^F/SOD^S heterodimers of wild-type SOD were detected, but active mutant homodimers and mutant/wild-type heterodimers were not. The absence of active mutant homodimers rules out the unlikely possibility that the reduced activity in any of the missense heterozygotes is caused only by the instability of heterodimers but not of homodimers. The expectation that reduced stability of mutant homodimers and mutant/wild-type heterodimers will be reflected as reduced or null activity in this assay is consistent with what is observed in a less extreme way for SOD^S dimers, which are less stable *in vivo* than SOD^F dimers (18, 19).

Dimer Dysequilibrium Model. These results are uniformly in accord with a model of dimer dysequilibrium in which

Table 2. Cu/Zn SOD activity in mutant heterozygotes of *Drosophila*

Genotype*	Type of allele	Cu/Zn SOD activity† Observed	Expected‡
Series 1			
Control (SOD^S/SOD^S)	—	(100.0)	
$x16/SOD^S$	Deletion	47.1	
$x39/SOD^S$	Deletion	58.1	
$h76/SOD^S$	Deletion	44.8	
	(Mean)	50.0	50
Series 2			
Control (SOD^S/SOD^F)		(100.0)	
$n58/SOD^F$	$Gly^{83} \rightarrow Asp$	10.1	
$n64/SOD^F$	$Gly^{42} \rightarrow Glu$	12.2	
$n83/SOD^F$	$His^{69} \rightarrow Tyr$	14.4	
$n145/SOD^F$	ND	14.2	
	(Mean)	12.7	50
Series 3			
Control (SOD^S/SOD^S)		(100.0)	
$n108/SOD^S$	$Gly^{49} \rightarrow Ser$	36.7	50

*See Table 1 and Fig. 2 for description of *SOD* alleles. Mutant heterozygotes were generated by outcrossing TM3-balanced stocks carrying the respective mutant *SOD* alleles to stocks bearing an appropriate SOD^+ allele.

†Extracts were made and assayed as described in *Materials and Methods*. Specific activity (units per mg of total protein) was determined in triplicate assays on at least two independent extracts. Values are given as percent of the control for that series. The control alleles in each series were chosen to allow electrophoretic resolution of all active dimeric forms of the enzyme in heterozygotes (see Table 1).

‡Expected activity if no mutant subunits are present or if mutant subunits are unstable and do not associate with wild-type subunits. This contrasts with the 25% value expected if subunit interactions are unaffected by the mutations in heterozygotes (see text for discussion).

unstable mutant subunits alter the steady-state equilibrium of stable, active dimers by impairing the function of wild-type subunits in heterozygotes. This model conforms at the molecular level to the dominant-negative mutation paradigm described by Herskowitz (29) and is formally analogous to the

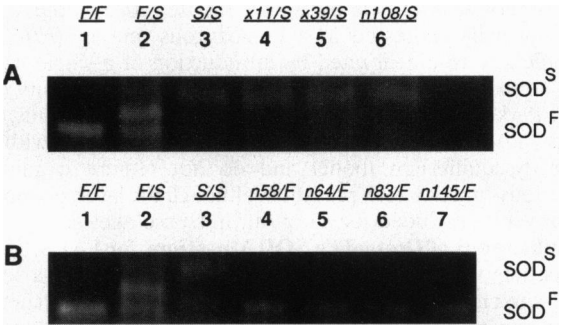

FIG. 4. Electrophoretic analysis of enzymatically active dimers formed in *SOD* mutant heterozygotes. Heterozygotes carrying a mutant *SOD* allele and the complementary SOD^S (*A*) or SOD^F (*B*) counter allele were analyzed for enzymatically active dimers by nondenaturing polyacrylamide gel electrophoresis. Equal amounts of total soluble protein extract (roughly equivalent to the amount extractable from a single adult) were applied to all lanes. The reduced activity of SOD^S homodimers (but not of SOD^S/SOD^F heterodimers) reflects the relative instability of this allozyme *in vivo* (18, 19).

mutant/wild-type subunit interactions observed in the multimeric enzyme aspartate transcarbamylase (30, 31). The absence of detectable mutant phenotype in *Drosophila SOD* heterozygotes probably arises as a consequence of the short lifespan of *Drosophila* coupled with the accumulative nature of oxygen radical-mediated pathology. Indeed, it would be surprising if FALS-type symptoms, which take decades to develop in humans, would be manifested in the short, 2- to 3-month lifespan of *Drosophila* ($t_{1/2}$ = 60 days for wild-type control strains and *SOD* mutant/SOD^+ heterozygotes under optimal laboratory conditions; see ref. 12).

A dominant gain-of-function model has been suggested to account for the dominant, midlife-onset neuropathology associated with *SOD* mutations in FALS patients (1) and more recently, in transgenic mice carrying a multicopy FALS transgene (10, 11). That *SOD* mutations in *Drosophila* are recessive with regard to neuropathological phenotype does not, by the same reasoning as above, render them inconsistent with this model. However, in contrast to recent experiments in mice wherein a multicopy mutant transgene elicited mutant symptoms

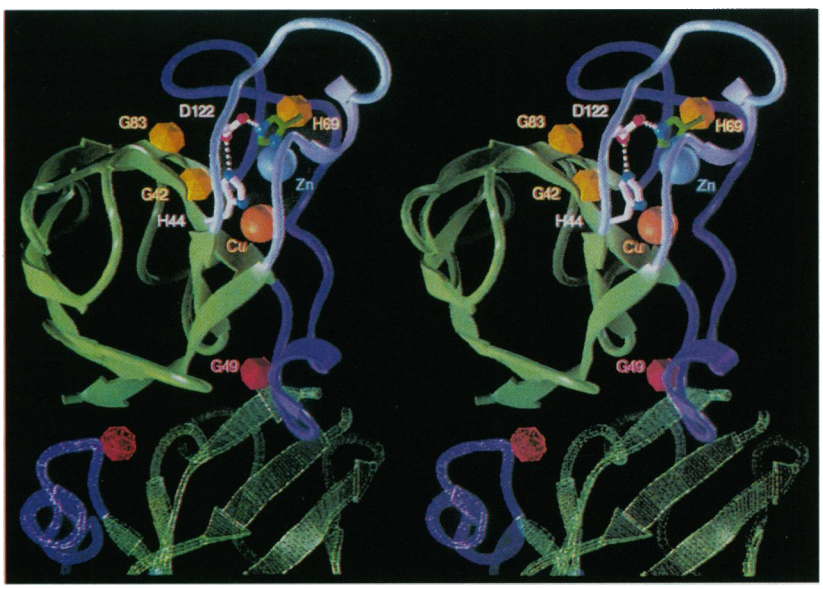

FIG. 3. Stereo ribbon diagram of the *Drosophila* SOD homology dimer model showing the subunit β-barrel fold with the position and interactions of single-site mutated residues. One complete subunit is shown (solid raster, top) with a portion of the second identical subunit (lines, bottom) to identify the dimer interface region. Viewed down a subunit β-barrel axis, the subunits are colored to identify the β-barrel (green arrows and tubes) and the electrostatic (light blue tubes) and Zn ligand loops (dark blue tubes) forming the active-site channel around the Zn (blue sphere) and catalytic Cu (gold sphere) ions. C^α positions are indicated for the three active-site mutation sites at Gly^{42}, Gly^{83}, and His^{69} (faceted orange spheres) and the dimer interface mutation site at Gly^{49} (faceted red sphere). The active-site Cu and Zn ions are connected by hydrogen bonds between Cu ligand His^{44} (white carbon and blue nitrogen bonds), buried Asp^{122} (white carbon and red oxygen bonds), and Zn ligand His^{69} (green carbon and blue nitrogen bonds). The active-site mutations are positioned to disrupt the critical connections between the active-site Cu and Zn ions by either removing the Zn-binding ligand ($His^{69} \rightarrow Tyr$), breaking the $His^{44} \cdots Asp^{122}$ hydrogen bond ($Gly^{42} \rightarrow Glu$), or breaking the $Asp^{122} \cdots His^{69}$ hydrogen bond ($Gly^{83} \rightarrow Asp$). The interface mutation ($Gly^{49} \rightarrow Ser$) would break a symmetric pair of main-chain hydrogen bonds across the dimer interface and force apart the subunits by steric collisions. Like the known human FALS mutations, these mutations all affect structurally conserved interactions in the human, bovine, and yeast SOD crystallographic structures that are expected to destabilize the dimer fold or the dimer assembly.

in an otherwise wild-type transgenic mouse (10, 11), the symptoms normally expressed in a homozygous mutant (*n108*) of *Drosophila* were ameliorated by introduction of a single native SOD^+ transgene expressing normal levels of SOD activity (ref. 17; T. Parkes, A.J.H., and J.P.P., unpublished data). Thus, our results with SOD mutations in *Drosophila* are consistent with the dimer dysequilibrium model and do not require a gain-of-deleterious-function interpretation, although the latter possibility cannot yet be excluded for all of our missense alleles.

Implications of *Drosophila* SOD Mutations for FALS. These results demonstrate that mutant subunits with one of a set of single-site changes that destabilize subunit or dimer structure confer negative effects on wild-type subunits with subsequent reduction of total SOD activity in mutant heterozygotes. This gives strong support to the conclusion that loss of SOD activity rather than gain of deleterious function is a principal underlying cause of neuropathology and other symptoms generated by these SOD mutations in *Drosophila*. None of the mutations producing the extreme negative subunit interaction generated experimentally in *Drosophila* have yet been identified in human populations. However, the locations of human FALS mutations in the SOD atomic structure indicate that they would have similar destabilizing effects, although of reduced severity. FALS mutations in human SOD principally affect motor neurons, a cell type lacking most cell cycle-dependent repair processes. In this regard, subunit-destabilizing SOD mutations in *Drosophila* are manifested in the largely postmitotic adult stage of development. The *Drosophila* adult may therefore be an especially useful *in vivo* experimental system for investigating the biological effects of FALS and other SOD mutations. Consistent with the potential application of the dimer dysequilibrium model to FALS, a recent paper (32) reports that affected members of a FALS family who carry the SOD $Gly^{93} \rightarrow Arg$ mutation have only 30% of normal SOD activity in erythrocytes and exhibit a significantly earlier onset of disease.

Several other important aspects of FALS genetics can be investigated with the *Drosophila* system. For example, some cases of FALS, although clearly familial, are not associated with mutations in *SOD* (1). Examining existing mutants of *Drosophila* which affect other components of oxygen-radical metabolism such as Mn SOD, catalase, or urate could identify other FALS candidate genes. Another common feature of FALS in humans is the wide variation in the age of onset and in the rate of progression of symptoms (33). Similar phenomena in *Drosophila* provide opportunity to elucidate the role of genetic background in phenotypic variation associated with *SOD* mutations. For example, we have recently selected independent phenotypic revertants arising from our original $cSOD^{n108}$ ($Gly^{49} \rightarrow Ser$) mutant stock. Although these revertants are still homozygous for the original *n108* allele (as determined by sequencing) and still lack detectable SOD activity, the phenotypic symptoms produced by the original $Gly^{49} \rightarrow Ser$ mutation are now fully or partially reverted to wild type (T. Parkes, B. Duyf, A.J.H., and J.P.P., unpublished data). Identifying the genetic and biochemical factors responsible for this striking suppression of symptoms normally associated with SOD mutations in *Drosophila* should have important etiological and therapeutic implications for FALS in humans.

We thank Roy Meidinger for SOD assays, I. Meinhertzhagen for help with histopathology, Brenda Duyf for technical assistance, Michael Pique for help with computer graphics, and Meena Hariharan for help with molecular modeling. This work was supported by the Natural Sciences and Engineering Research Council of Canada and The Medical Research Council of Canada (J.P.P. and A.J.H.), The Canadian ALS Society (G.L.B.), and the U.S. National Institutes of Health (J.A.T. and E.D.G.).

1. Rosen, D. R., Siddique, T., Patterson, D., Figlewicz, D. A., Sapp, P., *et al.* (1993) *Nature (London)* **362,** 59–62.
2. Deng, H.-X., Hentati, A., Tainer, J. A., Iqbal, Z., Cayabyab, A., Hung, W.-Y., Getzoff, E. D., Hu, P., Herzfeldt, B., Roos, R. P., Warner, C., Deng, G., Soriano, E., Smyth, C., Parge, H. E., Ahmed, A., Roses, A. D., Hallewell, R. A., Pericak-Vance, M. A. & Siddique, T. (1993) *Science* **261,** 1047–1051.
3. Borchelt, D. R., Lee, M. K., Slunt, H. S., Guarnieri, M., Xu, Z. S., Wong, P. C., Brown, R. H., Price, D. L., Sisodia, S. S. & Cleveland, D. W. (1994) *Proc. Natl. Acad. Sci. USA* **91,** 8292–8296.
4. Robberecht, W., Sapp, P., Viaene, M. K., Rosen, D., Mckenna-yasek, D., Haines, J., Horvitz, R., Theys, P. & Brown, R. (1994) *J. Neurochem.* **62,** 384–387.
5. Bowling, A. C., Schulz, J. B., Brown, R. H. & Beal, M. F. (1993) *J. Neurochem.* **61,** 2322–2325.
6. McCord, J. M. (1994) *Science* **266,** 1586–1587.
7. Gurney, M. E. (1994) *Science* **266,** 1587.
8. Beckman, J. S., Carson, M., Smith, C. D. & Koppenol, W. H. (1993) *Nature (London)* **364,** 584.
9. Lipton, S. A., Choi, Y.-B., Pan, Z.-H., Lei, S. Z., Chen, H.-S., V., Sucher, N. J., Loscalzo, J., Singel, D. J. & Stamler, J. S. (1993) *Nature (London)* **364,** 626–632.
10. Gurney, M. E., Pu, H., Chiu, A. Y., Dal Canto, M. C., Polchow, C. Y., Alexander, D. D., Caliendo, J., Hentati, A., Kwon, Y. W., Deng, H.-X., Chen, W., Zhai, P., Sufit, R. L. & Siddique, T. (1994) *Science* **264,** 1772–1776.
11. Ripps, M. E., Huntley, G. W., Hof, P. R., Morrison, J. H. & Gordon, J. W. (1995) *Proc. Natl. Acad. Sci. USA* **92,** 689–693.
12. Phillips, J. P., Campbell, S. D., Michaud, D., Charbonneau, M. & Hilliker, A. J. (1989) *Proc. Natl. Acad. Sci. USA* **86,** 2761–2765.
13. Campbell, S. D., Hilliker, A. J. & Phillips, J. P. (1986) *Genetics* **112,** 205–215.
14. Phillips, J. P. & Hilliker, A. J. (1990) *Adv. Genet.* **28,** 43–71.
15. Hilliker, A. J., Duyf, B., Evans, D. & Phillips, J. P. (1992) *Proc. Natl. Acad. Sci. USA* **89,** 4343–4347.
16. Staveley, B. E., Phillips, J. P. & Hilliker, A. J. (1990) *Genome* **33,** 867–872.
17. Reveillaud, I., Phillips, J. P., Duyf, B., Hilliker, A. J., Kongpachith, A. & Fleming, J. (1994) *Mol. Cell. Biol.* **14,** 1302–1307.
18. Lee, Y. M., Friedman, D. J. & Ayala, F. J. (1985) *Arch. Biochem. Biophys.* **241,** 577–589.
19. Lee, Y. M., Misra, H. P. & Ayala, F. J. (1981) *Proc. Natl. Acad. Sci. USA* **78,** 2052–2055.
20. Lindsley, D. L. & Zimm, G. (1992) *The Genome of Drosophila melanogaster* (Academic, New York).
21. Restifo, L. L. & White, K. (1990) *Adv. Insect Physiol.* **22,** 116–219.
22. Beauchamp, C. O. & Fridovich, I. (1971) *Anal. Biochem.* **44,** 276–287.
23. Seto, N. O. L., Hayashi, S. & Tener, G. M. (1987) *Nucleic Acids Res.* **15,** 10601.
24. Tainer, J. A., Getzoff, E. D., Beem, K. M., Richardson, J. S. & Richardson, D. C. (1982) *J. Mol. Biol.* **160,** 181–217.
25. Parge, H. E., Hallewell, R. A. & Tainer, J. A. (1992) *Proc. Natl. Acad. Sci. USA* **89,** 6109–6113.
26. Parge, H. E., Getzoff, E. D., Scandella, C. S., Hallewell, R. A. & Tainer, J. A. (1986) *J. Biol. Chem.* **261,** 16215–16218.
27. Getzoff, E. D., Tainer, J. A., Stempien, M. M., Bell, G. I. & Hallewell, R. A. (1989) *Proteins Struct. Funct. Genet.* **5,** 322–336.
28. Forman, H. J. & Fridovich, I. (1973) *J. Biol. Chem.* **248,** 2645–2649.
29. Herskowitz, I. (1987) *Nature (London)* **329,** 219–222.
30. Gibbins, I., Flatgaard, J. E. & Schachman, H. K. (1975) *Proc. Natl. Acad. Sci. USA* **72,** 4298–4302.
31. Robey, E. A. & Schachman, H. K. (1985) *Proc. Natl. Acad. Sci. USA* **82,** 361–365.
32. Orrell, R., de Belleroche, J., Marklund, S., Bowe, F. & Hallewell, R. (1995) *Nature (London)* **374,** 504–505.
33. Mulder, D. W., Kurland, L. T., Offord, K. P. & Beard, C. M. (1986) *Neurology* **36,** 511–517.